

Optical studies of electrochemically synthesized CdS nanowires

Vijay Kumar · Sunil Kumar · Sanjeev Kumar ·
S. K. Chakarvarti

Received: 3 March 2010/Accepted: 13 May 2010/Published online: 25 May 2010
© Springer Science+Business Media, LLC 2010

Abstract In this paper, electrochemical fabrication and characterization of CdS nanowires having diameter 100 and 200 nm is reported. Nano-channels in anodic alumina membrane were utilized as template. Morphological study of nanowires was made using Scanning electron microscopy (SEM). UV-visible absorption and laser induced time resolved photoluminescence (PL) spectroscopy were used for optical characterization. UV-visible absorption depicts that, there is slight increase in band gap of nanowires with decrease in diameter of nanowires. PL measurements indicate emission band peak of 435 and 420 nm in case of 200 and 100 nm wires respectively. These studies are very important regarding the synthesis and optoelectronic applications of CdS nanowires.

1 Introduction

In recent years, semiconductor nanowires have assumed fundamental interest because these structures with size confinement in two coordinates exhibit novel physical properties which make them suitable for potential applications in nanoscale electronics, optoelectronic devices, high-density magnetic memories, electrochemical and sensing devices [1–7]. The special properties of nanowires are due to high aspect ratio, quantum confinement effects and an extremely large surface to volume ratio relative to bulk materials. Among semiconductor materials, CdS is the most commonly studied material for functional nanodevices such as light emitting diodes, sensors, solar cells, photoconductors, thin film FETs and optoelectronic devices [8–14]. CdS is a well known direct band gap II–VI semiconductor with $E_g = 2.42$ eV at room temperature. So far, a variety of techniques such as physical vapor deposition [15], chemical solution transport growth [16, 17], solvothermal synthesis [18], sulfurization [19], microwave assisted growth [20], thermal evaporation [21] and electrodeposition [22, 23] have been used to synthesize CdS nanowires.

Template synthesis is an elegant chemical approach for the fabrication of nanostructures, in particular of nano-wires and tubules. It is a membrane based technology which makes use of porous templates as host materials for the deposition of desired materials such as metals, semiconductors, conducting polymers, carbon and other materials [23, 24 and references therein]. The nanostructures can remain inside the pores of templates or they can be freed and collected as an ensemble of free nanomaterials. Using electrodeposition method, we report here the template assisted growth of CdS nanowires within the nano-channels of anodic alumina

V. Kumar
Department of Physics, Punjab College of Engineering
and Technology, Lalu Mandi, District Mohali 140501, India
e-mail: nano_vijay1@yahoo.co.in

S. Kumar (✉)
Department of Physics, Maharishi Markandeshwar University,
Mullana, District Ambala, Haryana 133207, India
e-mail: sunilkumar32@gmail.com

S. Kumar
University College of Engineering, Punjabi University,
Patiala 147002, India
e-mail: sanjeevace_phy@yahoo.co.in

S. K. Chakarvarti
Manav Rachna International University (MRIU), Faridabad
121004, India
e-mail: skchakarvarti@gmail.com

membrane (AAM, Whatman USA) with pore diameter ~ 100 nm, 200 nm.

2 Experimental

Anodic alumina membranes (AAM) with pore diameters ~ 100 and 200 nm; purchased from Whatman, USA, were used as template. A gold layer of thickness ~ 100 nm was deposited onto one side surface of AAM to provide a good conductive contact using Jeol, fine sputter JFC 1100 sputter coater. The deposition of CdS within the pores of template was carried out at constant potential (1.62 V) for 30 min at room temperature (27 ± 1 °C) with an anode of pure Cd. The electrolyte solution used was 0.002 M $3\text{CdSO}_4 \cdot 8\text{H}_2\text{O}$ (98%) and 0.1 M Na_2SO_3 (99.9%). The pH value of the electrolyte was adjusted 2.5 using dilute H_2SO_4 . Figure 1 shows the current versus time response for electro-deposition of CdS nanowires of 100 nm (a) and 200 nm (b). The current versus time graph shows that the deposition of nanowires is not a steady state process. After applying the potential, the current dropped suddenly due to creation of diffusion layer within the pores of template and afterwards the current gradually increased during the growth of nanowires in the template and attained a steady state when the filling reached the top of template. As soon as caps start to cultivate on the top of structure, the current starts increasing slowly which increases rapidly with the increase of surface area of the caps due to over-deposition [25]. After the deposition was over, the AAM was dissolved in 1 M NaOH solution for 30 min followed by rinsing with double distilled water in order to retrieve the nanowires. Finally, the samples were dried at room temperature before being subjected to further characterization.

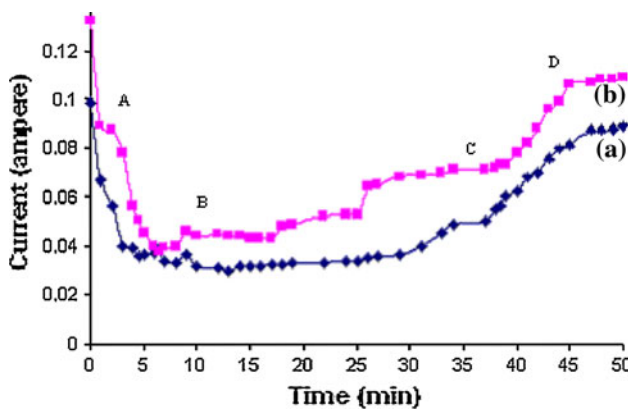


Fig. 1 Current versus time response for potentiostatic deposition of CdS nanowires of 100 nm (a) and 200 nm (b)

3 Result and discussion

3.1 Morphological properties

For morphological study, the rinsed and dried samples were mounted on specially designed aluminum stub with the help of double adhesive tape, coated with layer of gold–palladium alloy in JEOL, FINE SPUTTER JFC 1100 sputter coater and viewed under scanning electron microscope (JEOL JSM 6100) at an accelerating voltage of 10 kV. Figures 2 and 3 show the SEM photograph of CdS nanowires. The diameter of nanowires closely corresponds to the diameter of pores of the AAM. From the SEM figures, it is clear that the growth of nanowires is uniform and confined within the ordered pores of the AAM.

3.2 UV–visible absorption studies

The fundamental optical property of CdS nanowires investigated here is the absorption spectra at various wavelengths using UV–visible spectrophotometer. Figures 4 and 5 shows the absorption spectra of CdS nanowires of 100 and 200 nm respectively. The energy band gap of CdS nanowires is

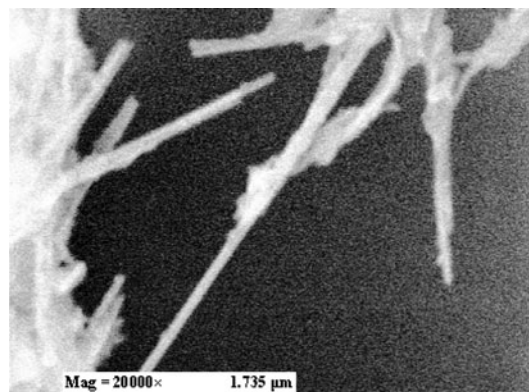


Fig. 2 SEM photographs of CdS nanowires (100 nm)

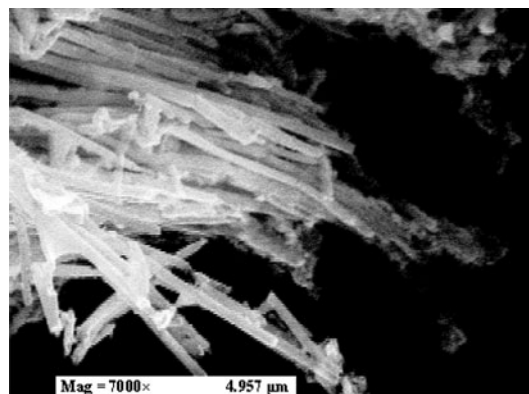


Fig. 3 SEM photographs of CdS nanowires (200 nm)

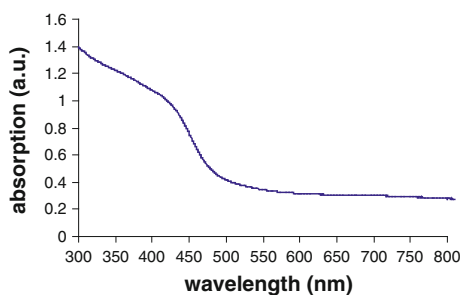


Fig. 4 Plot of absorption (α) versus wavelength (λ) for CdS nanowires (100 nm)

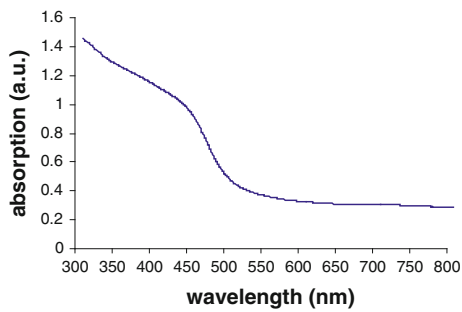


Fig. 5 Plot of absorption (α) versus wavelength (λ) for CdS nanowires (200 nm)

determined from absorption spectra using Tauc relation [26]:

$$\alpha h\nu = A(h\nu - E_g)^n,$$

where α , $h\nu$, E_g , n and A have their usual meanings.

The graphs between $(\alpha h\nu)^2$ versus $h\nu$ for CdS nanowires of 100 and 200 nm are shown in Figs. 6 and 7 respectively. The presence of single slope indicates the direct and allowed transitions. The extrapolation of straight line to $h\nu$ axis gives value of energy gap value of CdS nanowires. From the graph, the band gap in case of 200 nm wires comes out to be 2.46 and 2.51 eV in case of 100 nm nanowires. It is seen that there is not much change in the

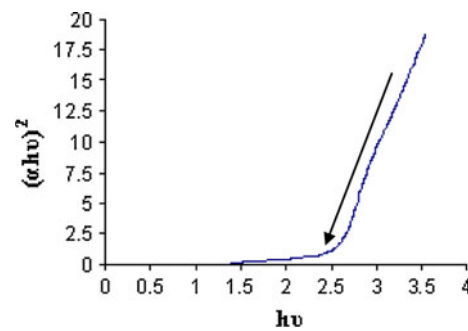


Fig. 7 Plot of $(\alpha h\nu)^2$ versus $h\nu$ (Tauc plot with dotted line is a theoretical fit) for CdS nanowires (100 nm)

band gap of nanowires when size changes from 200 to 100 nm.

3.3 Time resolved photoluminescence

Further, laser induced time resolved photoluminescence was used to study the photoluminescence spectra of 100 and 200 nm CdS nanowires. Nitrogen laser having pulse-width of 5–7 ns, average power of 10 kW, peak power of 1 MW and wavelength 337.1 nm is used to irradiate the CdS nano-/microstructures. High photon flux density of the Nitrogen laser is extremely useful to excite any type of defect states. The short-lived phosphorescence from the sample at an angle of 90° to the incident beam was collected by a fast photo-multiplier tube (PMT) through an assembly of monochromator and PMT.

The decay signals (Figs. 8 and 9) from the CdS nanowires were recorded for calculating emission wavelength of the nanowires. Photoluminescence investigation shows that the 200 nm CdS nanowires have an intensive and broad PL emission band peaked around 435 nm and with decrease in the size of CdS nanowires to 100 nm, only negligible variation is observed in the photoluminescence wavelength i.e. 420 nm. Photoluminescence in case of nanowires suggest that localized defects and excess S

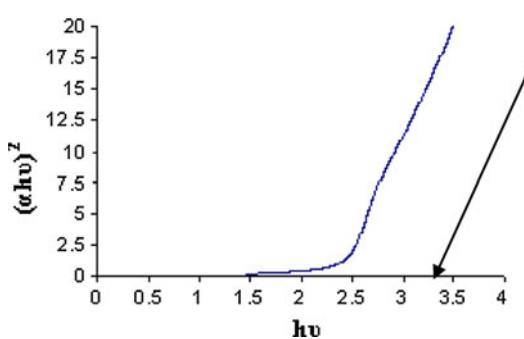


Fig. 6 Plot of $(\alpha h\nu)^2$ versus $h\nu$ (Tauc plot with dotted line is a theoretical fit) for CdS nanowires (200 nm)

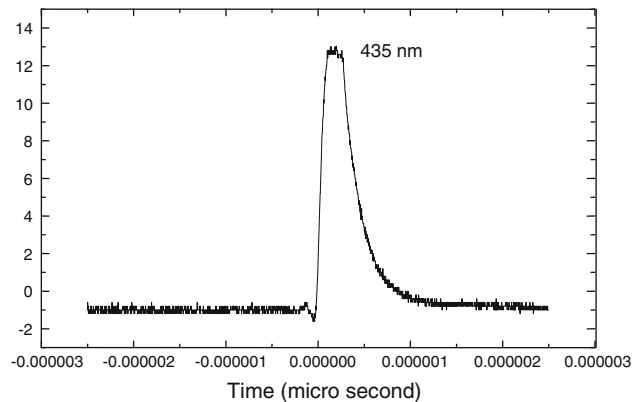


Fig. 8 Decay curve of 200 nm CdS nanowires

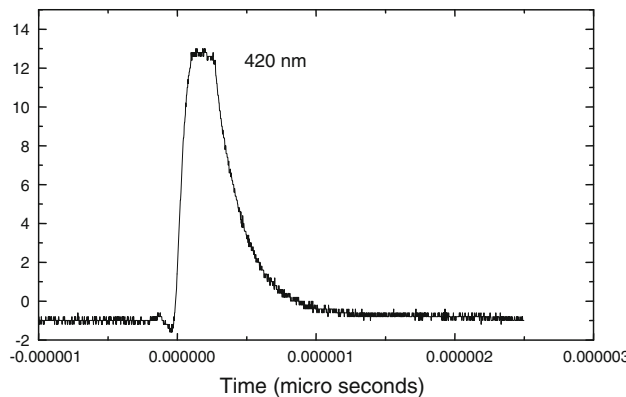


Fig. 9 Decay curve of 100 nm CdS nanowires

atoms existing in the CdS nanowires are responsible for this blue luminescence as no dopant had been added to the host CdS. In our earlier work regarding ZnO nanowires, defect related emission was observed at 590 nm [27].

4 Conclusion

CdS nanowires were fabricated using template synthesis, which proves to be cost effective technique for the production of wide range of nanostructures with specified geometry. SEM results indicate that the wires are uniform, dense and diameter corresponds to the pore diameter of template. An optical bandgap study also shows not much change in the band gap with decrease in diameter of nanowire. It is due to the fact that the diameter of the nanowires is very much greater than the bohr exciton radius and there is no confinement. The defect related emission is observed in this case of undoped CdS nanowires.

Acknowledgments We thank Mr. M.L. Sharma, Ex-Senior Scientific Officer, SAIF, Punjab University Chandigarh, for providing SEM facility and valuable suggestions, respectively.

References

1. D.H. Cobden, Nature **409**, 32 (2001)
2. C. Ma, D. Moore, J. Li, Z.L. Wang, Adv. Mater. **15**, 228–231 (2003)

3. G. Fasol, Science **272**, 1751 (1996)
4. C. Stafford, D. Baeriswyl, J. Buerki, Phys. Rev. Lett. **79**, 2863 (1997)
5. C. Hoppleer, W. Zwrger, J. Phys. Rev. B **59**, R7849–R7851 (1999)
6. G.A. Prinz, Science **282**, 1660–1663 (1998)
7. L. Samuelson, M.T. Bjork, K. Deppert, M. Larsson, B.J. Ohlsson, N. Paney, A.I. Persson, N. Skold, C. Thelander, L.R. Wallenberg, Physica-E **21**, 560–567 (2004)
8. M.E. Calixto, P.J. Sebastian, Sol. Energy Mater. Sol. Cells **59**, 65 (1999)
9. J. Levinson, F.R. Shepherd, P.J. Scanlon, W.D. Westwood, G. Este, M. Rider, J. Appl. Phys. **53**(2), 1193 (1982)
10. Y. Kang, D. Kim, Sol. Energy Mater. Sol. Cells **90**, 166–174 (2006)
11. X.F. Duan, Y. Huang, R. Agarwal, C.M. Lieber, Nature **421**, 241 (2003)
12. U. Pal, R. Silva-Gonalez, G. Martinez-Montes, M. Gracia-Jimenez, M.A. Vidal, Sh. Torres, Thin. Sol. Films **305**, 345 (1997)
13. X. Duan, C. Niu, V. Sahi, J. Chen, J.W. Parce, S. Empedocle, J.L. Goldman, Nature **425**, 274 (2003)
14. U. Woggon, S.V. Bogdanov, O. Wind, K.H. Schlaad, H. Pier, C. Klingshirn, P. Chatzigrastou, H.P. Fritz, Phys. Rev. B **48**, 11979–11986 (1993)
15. X.C. Wu, Y.R. Tao, J. Cryst. Growth **242**, 309–312 (2002)
16. J.H. Zhan, X.G. Yang, S.D. Li, D.W. Wang, Y. Xie, Y.T. Qian, J. Cryst. Growth **220**, 231–234 (2000)
17. H. Zhang, X. Ma, J. Xu, J. Niu, J. Sha, D. Yang, J. Cryst. Growth **246**, 108–112 (2002)
18. Q.Q. Wang, G. Xu, G.R. Han, J. Sol. State. Chem. **178**(9), 2680–2685 (2005)
19. J. Fan, T. Gao, G. Meng, Y. Wang, X. Liu, L. Zhang, Mater. Lett. **57**, 656–659 (2002)
20. N. Yonghong, X. Ma, J. Hong, Z. Xu, Mater. Lett. **58**, 2754–2756 (2004)
21. J. Zhang, Y. Yang, F. Jiang, J. Li, B. Xu, S. Wang, X. Wang, J. Cryst. Growth **293**, 236–241 (2006)
22. I. Enculescu, M. Sima, V. Ghordanescu, M. Secu, Chalcogenide Lett. **2**(2), 9–15 (2005)
23. S.K. Chakarvarti, J. Vetter, Rad. Meas. **29**(2), 149–159 (1998)
24. A. Huczko, Appl. Phys. A **70**, 365–376 (2000)
25. Sanjeev. Kumar, Rajesh. Kumar, Shyam. Kumar, S.K. Chakarvarti, Curr. Sci. **87**, 642 (2004)
26. W.E. Mahmoud, H.M. El-Mallah, Phys. D. Appl. Phys. **42**, 035502 (2009)
27. V. Kumar, S. Kumar. S. K. Chakarvarti (2010) J. Mat. Sci Mater. Electronics, Springer + Business Media